Atmos. Chem. Phys. Discuss., https://doi.org/10.5194/acp-2019-239
Manuscript under review for journal Atmos. Chem. Phys.
Discussion started: 18 March 2019

Atmospheric Chemistry and Physics
Discussions
Open Access

Implications of constant CFC-11 concentrations for the future ozone layer

Martin Dameris, Patrick Jöckel, Matthias Nützel

Deutsches Zentrum für Luft- und Raumfahrt, Institut für Physik der Atmosphäre, Oberpfaffenhofen, Germany

Correspondence to: Martin Dameris (martin.dameris@dlr.de)

Abstract. This investigation is motivated by the results presented by Montzka et al. (2018). They discussed a strong deviation of the assumed emissions of chlorofluorocarbon-11 (CFC-11, $CFCl_3$) in the past 15 years, which indicates a violation of the Montreal Protocol for the protection of the ozone layer. A Chemistry-Climate Model (CCM) study is performed, investigating the consequences of a constant CFC-11 surface mixing ratio for stratospheric ozone: In comparison to a reference simulation (REF-C2), where a decrease of the CFC-11 surface mixing ratio of about 50% is assumed from the early 2000s to the middle of the century, a sensitivity simulation (SEN-C2-fCFC11) is carried out where after the year 2002 the CFC-11 surface mixing ratio is kept constant until 2050. Differences between these two simulations are shown. These illustrate possible effects on stratospheric ozone. The total column ozone (TCO) in the 2040s (i.e. the years 2041-2050) is in particular affected in both polar regions in winter and spring. At the end of the 2040s maximum discrepancies of TCO are identified with reduced ozone values of up to around 30 Dobson Units (in the order of 10%) in the SEN-C2-fCFC11 simulation. An analysis of the respective partial column ozone (PCO) for the stratosphere indicates that strongest ozone changes are calculated for the polar lower stratosphere, where they are mainly driven by the enhanced stratospheric chlorine content and associated heterogeneous chemical processes. Furthermore, it turns out that the calculated ozone changes, especially in the upper stratosphere, are smaller than expected. In this altitude region the additional ozone depletion due to the catalysis by reactive chlorine is compensated partly by other processes related to enhanced ozone production or reduced ozone loss, for instance from nitrous oxide (NO_x).

1 Introduction

The estimation of the future evolution of the ozone layer is a central part of the UNEP/WMO Scientific Assessment of Ozone Depletion. For that reason Chemistry-Climate Models (CCM) are carrying out long-term simulations (for several decades). These models are performing comprehensive numerical simulations under well-defined boundary conditions which are prescribing possible future changes of ozone depleting substances (ODSs), particularly those related to changes of chlorofluorocarbon (CFC) concentrations. In recent years, model guidelines have been defined, to facilitate the intercomparison of CCM results from different modelling groups world-wide. For instance, in 2012 the Chemistry-Climate Model Initiative (CCMI), under the umbrella of IGAC/SPARC, defined the boundary conditions for the next round of coordinated reference (REF) and sensitivity (SEN) simulations (Eyring et al., 2013). The boundary conditions for the CCM simulations consider not only the expected changes of ODSs according to the regulations of the Montreal Protocol and its amendments, but also the influence of different climate change scenarios. Here, the greenhouse gas concentrations for the Representative Concentration Pathways (RCPs) adopted by the IPCC for its 5th Assessment Report (AR5) in 2014 (van Vuuren et al., 2011) were recommended. The suggested reference simulation for the future (REF-C2) assumes full compliance with the Montreal Protocol, expecting more or less no further production of CFCs.

More recently the respective CCM results were presented and discussed in several scientific papers, for instance by Dohmse et al. (2018). Among other things the question of ozone recovery was investigated, and how the speed of recovery and the return date are affected by the expected decrease of ODSs and by climate change. The results of the CCM simulations were taken into account as the foundation for the latest WMO ozone report (WMO, 2019).

During the preparation phase of WMO (2019) a paper by Montzka et al. (2018) was published, indicating a clear deviation of the expected surface concentration of CFC-11 ($CFCl_3$) in the past 15 years. Observational datasets discussed by Montzka et al. (2018; M18) showed that (1) in the last 10 years (until 2017) the decline of CFC-11 surface mixing ratios was obviously much slower than expected (see Figure 1a in M18); (2) the decline of CFC-11 surface mixing ratios was nearly constant from 2002 to 2012, whereas in the following years the decrease of CFC-11 surface mixing ratios decelerated (here until 2017; see Figure 1b in M18). The measurements indicated increased CFC-11 emissions after 2012 (see Figure 2a in M18; see also Figure ES-2 in WMO, 2019). Montzka and colleagues (M18) mentioned that these observations imply “a gap in our understanding of CFC-11 sources and sinks since the early 2000s”.

Based on these findings a significant impact on the recovery of the ozone layer seems to be possible, in particular, if CFC-11 emissions do not decline as previously anticipated (e.g. Daniel and Velders et al., 2011; Carpenter and Reimann et al., 2014). Therefore the assumption of decreasing CFC-11 surface mixing ratio in future by CCMI is partly questionable. Currently the evolution of CFC-11 emissions in the future is unclear: Here, we employ a simplified scenario of future CFC-11 emissions in a sensitivity simulation (SEN-C2-fCFC11) through constant surface mixing ratios from 2002 onwards. Although M18 hinted that the additional CFC-11 emissions might be released in eastern Asia, we do not impose any specific regional features due to long lifetime of CFC-11 (e.g. Rigby et al., 2013). In comparison with the reference simulation (REF-C2) the sensitivity simulation allows us to investigate the potential impact of previously unaccounted CFC-11 emissions. The sensitivity simulation covers the period from 2002 to 2050. It allows a rough estimation of the additional possible ozone loss under unchanged CFC-11 emissions in the coming years and how it may impact the timing of full recovery of the ozone layer.

After a short description of the used CCM and the analyzed model simulations (REF-C2 and SEN-C2-fCFC11) in the next section (Sec. 2), the CCM results are presented in Section 3. For the results, we focus on changes of total column ozone and partial stratospheric columns in specific geographical regions and seasons. Finally, the discussion and conclusion will be presented at the end of this paper.

2 Description of the model and simulations

For this study, the CCM EMAC (abbreviation stands for "European Centre for Medium-Range Weather Forecasts – Hamburg (ECHAM)/Modular Earth Submodel System (MESSy) Atmospheric Chemistry model") is used in the version 2.52 and is operated at a resolution of T42L90MA corresponding to a quadratic Gaussian grid of approx. 2.8 by 2.8 degrees in latitude and longitude with 90 levels up to 0.01 hPa. More details were presented by Jöckel et al. (2016).

The joint IGAC/SPARC Chemistry-Climate Model Initiative (CCMI) proposed several reference and sensitivity simulations among others for CCM studies. The aim was to support upcoming ozone and climate assessment reports. In this connection an internally consistent simulation from the past into the future between 1960 and 2100 has been suggested (Eyring et al., 2013). This transient reference simulation, i.e. REF-C2, as used in this study, is forced by trace gas projections and prescribed sea surface temperatures (SSTs) and sea ice concentrations (SICs). The projection component of REF-C2 uses greenhouse gas concentrations (i.e. CO_2, CH_4, and N_2O) that follow the Intergovernmental Panel on Climate Change (IPCC) Coupled Model Intercomparison Project Phase 5 (CMIP5) Representative Concentration Pathways 6.0 (RCP 6.0) scenario (van Vuuren et al., 2011). Monthly mean global SST and SIC data, which were simulated by the climate model HadGEM2 with an interactive ocean (Hadley Centre Global Environment Model version 2, data used for the RCP6.0 scenario; see Jones et al., 2011), are used as boundary conditions for the REF-C2 simulation.

For this study, in addition to the REF-C2 simulation (for more details see Jöckel et al., 2016; here it is the "RC2-base-04" reference simulation), a specific sensitivity simulation (SEN-C2-fCFC11) is designed to address the possible consequences of constant emissions of CFC-11, which lead to constant CFC-11 surface mixing ratios and therefore affect the chlorine content of the stratosphere after some years. In both EMAC simulations mixing ratios of ODSs (CFCs: $CFCl_3$, CF_2Cl_2, CH_3CCl_3, CCl_4; HCFCs: CH_3Cl, CH_3Br; Halons: CF_2ClBr, CF_3Br) in the lowest model layer are adapted by Newtonian relaxation to observed or projected surface mixing ratios (Kerkweg et al., 2006). In the REF-C2 simulation the mean CFC-11 surface mixing ratio in the year 2002 is 258.3×10^{-12} mol/mol (see Table 5A-3 in Daniel and Velders et al., 2011) and it is significantly reduced by more than 50% (127.2×10^{-12} mol/mol) in the year 2050 (i.e. the mixing ratio of the baseline (A1) scenario; WMO, 2011). The 2050 value is projected under the assumption of full compliance with the Montreal Protocol. Apart from one point the sensitivity simulation (SEN-C2-fCFC11) is identical to the reference simulation (REF-C2): for simplicity, in the sensitivity simulation the CFC-11 mean surface mixing ratio is kept constant at 258.3×10^{-12} mol/mol after the year 2002, whereas they decline in the reference simulation. In the sensitivity simulation we do not emphasize specific regions regarding outstanding changes of the CFC-11 surface mixing ratio, e.g. in eastern Asia. The modified CFC-11 boundary condition in the SEN-C2-fCFC11 simulation should cause a change of the stratospheric chlorine loading after about 10-15 years (e.g. Engel et al., 2002). The SEN-C2-fCFC11 simulation covers the period from 2002 to 2050.

3 Presentation of CCM results

3.1 Reactive chlorine

Based on the prescribed changes of the CFC-11 boundary conditions the stratospheric content of reactive chlorine compounds ($ClO_x = Cl + ClO + OClO + 2ClOOCl + 2Cl_2 + HOCl$) is expected to change. In Figure 1 the simulated change (i.e. SEN minus REF) of reactive chlorine mixing ratios with time is shown for the lower stratospheric (LS, near 50 hPa) and the upper stratosphere (US, near 2 hPa). Because these two model simulations are both operated in a "free-mode" (i.e. not having the same meteorology), the year-to-year difference (grey) curve as shown in Figure 1 (and also in other figures shown afterwards) is indicating the possible range of interannual fluctuation. Obviously it takes about 15 years of time (as expected) before the ClO_x values of the two EMAC simulations clearly diverge from each other. At the end of the SEN-C2-fCFC11 simulation (i.e. 2050) the resulting absolute (mean) difference in EMAC arises to an approximately $6x10^{-12}$ mol/mol increase in the LS and about $50x10^{-12}$ mol/mol in the US compared to the REF-C2 simulation. This vertical dependence of the changes of chlorine mixing ratios is related to the reference ClO_x profile in EMAC, which displays a distinct maximum at about 2-3 hPa (not shown). It turns out that in the US (above 30 km) in the 2040s (i.e. the time period from 2041 to 2050) the amount of chemically active chlorine species (ClO_x) in the SEN-C2-fCFC11 simulation is roughly 17-21% larger than in the REF-C2 simulation.

3.2 Total and partial ozone columns

The impact of the enhanced atmospheric ClO_x content due to constant CFC-11 surface mixing ratio after 2002 on total column ozone (TCO) is shown in Figure 2. It illustrates the differences between the REF-C2 and the SEN-C2-fCFC11 simulation of the mean annual cycle for the last decade of the SEN-C2-fCFC11 simulation depending on the geographical latitude. The largest changes of TCO are found in both polar regions: in particular in the Northern Hemisphere during winter (December, January, February) and in the Southern Hemisphere in late winter (August) to early spring (September, October). In the SEN-C2-fCFC11 simulation the TCO values are clearly reduced by up to about 30 Dobson Units (DU) (in the order of 10%) in comparison to the REF-C2 simulation. During other times of the year and in other latitudinal regions the identified TCO changes are much smaller. They are mostly below ±5 DU.

A closer look at the near global mean (60° S – 60° N) temporal behavior of TCO (Figure 3) indicates a recovery of the ozone layer in both simulations (upper part of the figure). The results of the SEN-C2-fCFC11 simulation are showing slightly smaller TCO values in comparison to REF-C2 and a slightly flatter slope of the linear trend line. This is supported by the TCO difference (lower part of the figure) which indicates a small reduction of the TCO (in SEN-C2-fCFC11) of about up to

3 DU (in the order of 1%) until 2050. This effect can be rated as negligible in comparison with the expected annual fluctuations in this region. Therefore in the following we focus on the analyses of the polar regions, in particular on the Antarctic region in September.

In the Southern Hemisphere polar region (70° S – 90° S) in September obvious ozone changes can be identified (Figure 4). The mean differences of the TCO between the 2000s and the end of the simulation amount to about 20 DU, indicating that the mean September ozone values in the SEN-C2-fCFC11 simulation are about 10% lower than in the REF-C2 simulation. The temporal evolution of TCO differences and the size of the ozone disturbance found in the Northern Hemisphere polar region in January have the same order of magnitude (not shown), but the signal is very noisy because of the stronger dynamic variability.

Now we are looking in more detail into stratospheric partial columns of ozone (PCO), for the upper stratosphere (US) and the lower stratosphere (LS) – i.e. columns below and above 10 hPa, respectively – for the Antarctic region in September. Figure 5 shows the PCO differences for the US (top part) and LS (bottom part) between the SEN-C2-fCFC11 and the REF-C2 simulation. Both are showing the expected negative trend, indicating lower values at the end of the SEN-C2-fCFC11 simulation in the late 2040s. The mean PCO changes for the US with about 2 DU are much smaller than those calculated for the LS (about 20 DU). The temporal evolution of the PCO differences in the LS show almost similar results as found for the TCO differences (Figure 4): in the SEN-C2-fCFC11 simulation the TCO is reduced by about 20 DU until the year 2050. The strongest signature of ozone change found in the polar LS points to the importance of heterogeneous chemical processes. Viewing the vertical profile of the differences of net-ozone production rates of ClO_x between the REF-C2 and the SEN-C2-fCFC11 simulation in the 2040s clearly indicates an absolute minimum (i.e. less net-ozone production in SEN-C2-fCFC11) at around 50 hPa and another relative minimum at about 1.5 hPa in September (Figure 6, right part; see explanation in Section 3.3). Complementary, looking at the PCO changes in middle and lower latitude regions (60° S – 60° N, not shown) the partial column differences clearly show that the small ozone differences detected in the TCO (lower part of Figure 3) are affected by ozone reductions of similar magnitudes in the US and the LS, displaying only small contributions to the TCO.

3.3 Stratospheric ozone budget

In the following, a more detailed analysis of individual ozone production and loss processes is carried out. This ozone budget analysis is used to investigate the role of separate chemical cycles and reactions, which are responsible for ozone production and loss in the stratosphere. For this analysis the MESSy tool StratO3Bud (cf. Meul et al., 2014, based on Jöckel et al., 2006) is employed. The respective reactions responsible for stratospheric ozone production (attributed to photolysis hυ, HO_2 and CH_3O_2) and loss (attributed to O_x, NO_x, HO_x, ClO_x and BrO_x) are described by Meul et al. (2014, see their Table 2). In Figure 6 the results of this budget analysis are shown as changes of the ozone production rate between the SEN-C2-fCFC11 and the REF-C2 simulation $\left(\Delta P_{SEN-REF}^{prc}\right)$ with respect to the total production rate in the REF-C2 simulation. The explicit formula for calculating the changes of the ozone production rate at a certain level is given as

$$\Delta P_{SEN-REF}^{prc}(lev) = \frac{\sum_{lat\,\in\,R} P_{SEN}^{prc}(lat,lev) - \sum_{lat\,\in\,R} P_{REF}^{prc}(lat,lev)}{\sum_{lev}\sum_{lat\in R} P_{REF}^{tot}(lat,lev)}$$

Here, P denotes the temporal mean and zonally summed ozone production rate (molecules/s). The subscript denotes the respective simulations and the “prc” superscript denotes, which process (hυ, HO_2, CH_3O_2, O_x, NO_x, HO_x, ClO_x, and BrO_x) is analyzed. Loss cycles are regarded as negative production rates. Further, the superscript “tot” denotes the sum of all positive production rates (namely of hυ, HO_2, CH_3O_2) and the summation goes over all latitudes, which lie in the respective latitudinal band R. Here we show profiles of $\Delta P_{SEN-REF}$ for the annual global mean and the Southern Hemisphere polar region (70°S – 90°S) during September 2041–2050. In the Antarctic spring season (Figure 6, right part) obviously the enhanced content of reactive chlorine in the SEN-C2-fCFC11 simulations is responsible for the intensified ozone loss in the LS (around 50 hPa) and US (around 1.5 hPa). In the LS also ozone loss through the BrO_x cycle is enhanced, probably related to the enhanced chlorine loading as ozone loss due to the reaction of BrO with ClO is attributed to the BrO_x cycle (cf. Meul et al., 2014). On the other hand, as a consequence of more available chlorine, other loss cycles or production processes show a tendency to compensate the enhanced ozone destruction by chlorine. For instance the catalytic NO_x-cycle shows some balancing in the altitude region between about 19 km (50 hPa) and the stratopause (about 0.7 hPa). This means that in the 2040s the ozone depletion by NO_x is clearly reduced (i.e. a relative ozone production) in the SEN-C2-fCFC11 compared to the REF-C2 simulation above about 40 hPa. The results with respect to global annual means of the ozone production and loss shown in Figure 6 (left part) indicate that below about 50 hPa no obvious changes are detected. Above 20 km the ozone loss is strongly affected by reactive chlorine and again some compensation effects in the US due to other competing ozone loss cycles are clearly identified. The positive values with respect to the photolysis rates indicate a slight downward shift of the ozone layer (ozone maximum) to lower altitudes. Probably, this is due to enhanced ozone loss through chlorine at higher altitudes, which allows more UV radiation to reach lower altitudes, where this additional radiation in turn causes higher photolysis rates.

To check the possible impact of temperature changes due to enhanced CFC-11 concentrations on ozone chemistry we have analyzed the overall temperature trends in the US (near 1 hPa) and LS (near 50 hPa) and also the differences between REF-C2 and SEN-C2-fCFC11. The global annual mean long-term temperature behavior in the REF-C2 simulation is indicating a cooling of about 1 K in the LS and of about 3 K in the US from the early 2000s until to the year 2050. The temperature difference between REF-C2 and SEN-C2-fCFC11 amount to an additional cooling of about 0.3 K in the US in the SEN-C2-fCFC11 simulation, whereas no obvious change in the long-term behavior can be identified in the LS (not shown).

To take a closer look to the Southern Hemisphere polar region in spring, the REF-C2 simulation is indicating a clear cooling trend of about 4 K in the US (near 1 hPa) until 2050, whereas no obvious trend can be identified in the LS (not shown). With respect to temperature differences of SEN-C2-fCFC11 and REF-C2, the US does not show a clear change, whereas in the LS the SEN-C2-fCFC11 simulation suggests some additional cooling from the early 2000s until 2050 by about 2 K. However, this difference is superposed by large interannual fluctuations.

With this in mind we can try to value the calculated ozone differences in the SEN-C2-fCFC11 simulation in comparison to REF-C2. In the global mean US, on the one hand enhanced chlorine mixing ratios are leading to enhanced ozone depletion by the catalytic ozone destruction cycle; on the other hand the extra cooling is known to create a reduction of the ozone depletion rates by gas-phase chemistry (e.g. Haigh and Pyle, 1982). It turned out that the net effect here is slightly negative, i.e. indicate that ozone differences between REF-C2 and SEN-C2-fCFC11 in the US are dominated by the enhanced chlorine content. In the global mean LS, where no clear cooling is calculated, the smaller ozone values are therefore mainly caused by the enhanced chlorine content.

Looking closer at the South polar region in spring, it is obvious that in the US again the enhanced chlorine content is mostly responsible for the slightly reduced PCO in the SEN-C2-fCFC11 simulation (Figure 5, upper part). In the LS, where heterogeneous chemical processes are the most important drivers of ozone changes, the enhanced chlorine mixing ratios intensify the ozone destruction. This leads to significantly reduced PCO over the time (Figure 5, lower part) which eventually leads to the indicated (slight) extra cooling of the polar lower stratosphere in spring. A first analysis of Polar Stratospheric Cloud (PSC) statistics for the REF-C2 and SEN-C2-fCFC11 simulation displayed no considerable trend in the PSC surface area (not shown). Therefore we cannot identify any hint for enhanced chlorine activation.

4 Discussions and Conclusion

After the detection of an unexpected and persistent increase in global emissions of CFC-11 (Montzka et al., 2018) it is still unclear how these emissions will further develop and how these emissions will affect the recovery of the ozone layer. For that reason a simplified study based on CCM simulations is conducted to estimate roughly the implications of a constant mean CFC-11 surface mixing ratio for ozone depletion instead of reducing CFC-11 in the next decades. To keep things simple we do not consider regional differences with respect to CFC-11 emissions in our sensitivity simulation. From our point of view considering regional differences would not have relevant effects on the presented results because of the long lifetime of CFC-11 (e.g. Rigby et al., 2013; Engel and Rigby et al., 2019) , which leads to global mixing (Hoffmann et al., 2014). This study aims to estimate the order of magnitude of ozone changes due to constant CFC-11 surface mixing ratios in the coming years. In our view such a simplified approach is justified since there are many uncertainties with respect to the future evolution of CFC-11 emissions; currently a more precise approach is almost impossible. Therefore, the presented results should not be taken as a solid prediction of future conditions. They should turn the view to the potential impact of unchanged CFC-11 surface mixing ratio on the ozone layer.

The presented results indicate that mostly the ozone layer over the Arctic and Antarctic is significantly affected by the prescribed CFC-11 surface mixing ratio change. In our case, at the end of the SEN-C2-fCFC11 simulation the impact on TCO culminates in a maximum ozone decrease of up to 30 DU in both polar regions (Figure 2). The calculated ozone changes at middle latitude and tropical regions are surprisingly small (around less than ±5 DU) and therefore are mostly not statistically significant in the sense that the range of variability is in the same order of magnitude. It turns out from our analyses that the strengthened ozone depletion by enhanced chlorine is partly compensated by other ozone depleting catalytic cycles (e.g. NO_x) and other molecules (e.g. HO_2). For the global mean picture, there is no big TOC difference visible, as the effects of ozone production and loss processes are nearly cancelling. In the polar regions, although there are also compensating effects, the signal is noteworthy in spring (e.g. about 20 DU for the Antarctic region).

Finally, we present a simple estimate for the possible shift of the closure of the ozone hole over Antarctica due to the effect of constant CFC-11 surface mixing ratios after the year 2002. For this we are using the temporal evolution of the total stratospheric ClO_x loading in the REF-C2 (started in the middle of the 20th century) and the SEN-C2-fCFC11 simulation. In the REF-C2 simulation ClO_x values are strongly increasing from 1960 onwards and are highest at the end of the 1990s. Starting in the 2000s ClO_x is decreasing. The 1980 value of the REF-C2 simulation can be regarded as a reference for chlorine conditions before the ozone hole appeared. This “pre-ozone hole” chlorine content is reached again around the year 2050 in the REF-C2 simulation. By extrapolating the linear regression line of the ClO_x content (for 2017 to 2050) of the SEN-C2-fCFC11 simulation (not shown) into the future, we estimate, that a pre-ozone hole, i.e. “1980”, ClO_x loading is likely to be reached before 2070. Therefore we can roughly estimate a maximum delay of the closure of the ozone hole of somewhat less than 20 years. Considering that Dohmse et al. (2018) determined the closure date for the ozone hole by the year 2060 (the multi-model mean for the analyzed REF-C2 simulations) and that the one sigma standard deviation is in the range of about ±5 years (see also Figure 4.22 by Langematz and Tully et al., 2019), this indicates that the calculated effects of constant CFC-11 surface mixing ratio could have a non-negligible effect on the closure date of the ozone hole. For the Arctic region enhanced stratospheric chlorine content means that there is the possibility of strong ozone depletion under specific dynamic conditions (i.e. a stable and cold polar vortex until March) for a slightly longer time period.

The presented results do not show very dramatic consequences for the global mean ozone layer due to the unchanged CFC-11 surface mixing ratio for the next years, but indicate relevant changes in the polar regions in winter and spring. In the light of our results showing chemical feedback processes, which are diluting their effects in parts, the compliance of the guidelines of the Montreal Protocol is absolutely necessary and exceptions should not be allowed. Without a further strong regulation of the CFC-11 and other ODS emissions (e.g. Laube et al., 2014; Hossani et al., 2017), this could affect significantly the recovery of the ozone layer including the timing of the closure of the ozone hole – and this should be avoided!

Code and data availability. The Modular Earth Submodel System (MESSy) is continuously developed and applied by a consortium of institutions. The usage of MESSy and access to the source code is licensed to all affiliates of institutions, which are members of the MESSy Consortium. Institutions can become a member of the MESSy Consortium by signing the

MESSy Memorandum of Understanding. More information can be found on the MESSy Consortium Web-site (http://www.messy-interface.org).

Author contributions. Both simulations were set-up and carried out by P.J. with support of M.D.; M.D. structured and composed the manuscript. The author team analyzed jointly the model data and compiled the results and all three authors contributed to the manuscript.

Competing interests. The authors declare that they have no conflict of interest.

Acknowledgements. The work described in this paper has received some funding from the Initiative and Networking Fund of the Helmholtz Association through the project "Advanced Earth System Modelling Capacity (ESM)". In addition, the authors acknowledge financial support from the DLR internal project KliSAW (Klimarelevanz von atmosphärischen Spurengasen, Aerosolen und Wolken), and the Research Unit SHARP by the Deutsche Forschungsgemeinschaft (DFG). The model simulations have been performed at the German Climate Computing Centre (DKRZ) through support from the Bundesministerium für Bildung und Forschung (BMBF). We used the NCAR Command Language (NCL) for data analysis and to create some of the figures of this study. NCL is developed by UCAR/NCAR/CISL/TDD and available on-line: http://dx.doi.org/10.5065/D6WD3XH5. We furthermore thank all contributors of the project ESCiMo (Earth System Chemistry integrated Modelling), which provide the model configuration and initial conditions. We acknowledge the World Climate Research Programme's Working Group on Coupled Modelling, which is responsible for CMIP, and we thank the HadGEM climate modelling group for producing and making available their model output. For CMIP the US Department of Energy's Program for Climate Model Diagnosis and Intercomparison provides coordinating support and led development of software infrastructure in partnership with the Global Organization for Earth System Science Portals.

References

Carpenter, L. J., and Reimann, S. (Lead Authors), Burkholder, J. P., Clerbaux, C., Hall, B. D., Hossaini, R., Laube, J. C., and Yvon-Lewis, S. A.: Update on Ozone-Depleting Substances (ODSs) and other gases of interest to the Montreal Protocol, Chapter 1 in Scientific Assessment of Ozone Depletion: 2014, Global Ozone Research and Monitoring, Project–Report No. 55, World Meteorological Organization, Geneva, Switzerland, 2014.

Daniel, J. S., and Velders, G. J. M. (Coordinating Lead Authors), Morgenstern, O., Toohey, D. W., Wallington, T. J., Wuebbles, D. J., Akiyoshi, H., Bais, A. F., Fleming, E. L., Jackman, C. H., Kuijpers, L. J. M., McFarland, M., Montzka, S. A., Ross, M. N., Tilmes, S. and Tully, M. B.: A Focus on Information and Options for Policymakers, Chapter 5 in Scientific Assessment of Ozone Depletion: 2010, Global Ozone Research and Monitoring Project-Report No. 52, 516 pp., Geneva, Switzerland, 2011.

Dhomse, S., Kinnison, D., Chipperfield, M. P., Cionni, I., Hegglin, M., Abraham, N. L., Akiyoshi, H., Archibald, A. T., Bednarz, E. M., Bekki, S., Braesicke, P., Butchart, N., Dameris, M., Deushi, M., Frith, S., Hardiman, S. C., Hassler, B., Horowitz, L. W., Hu, R.-M., Jöckel, P., Josse, B., Kirner, O., Kremser, S., Langematz, U., Lewis, J., Marchand, M., Lin, V., Mancini, E., Marécal, V., Michou, M., Morgenstern, O., O'Connor, F. M., Oman, L., Pitari, G., Plummer, D. A., Pyle, J. A., Revell, L. E., Rozanov, E., Schofield, R., Stenke, A., Stone, K., Sudo, K., Tilmes, S., Visioni, D., Yamashita, Y., Zeng, G.: Estimates of ozone return dates from Chemistry-Climate Model Initiative simulations, Atmos. Chem. Phys., 18, 8409–8438, https://doi.org/10.5194/acp-18-8409-2018, 2018.

Engel, A., Strunk, M., Muller, M., Haase, H. P., Poss, C., Levin, I., and Schmidt, U.: Temporal development of total chlorine in the high-latitude stratosphere based on reference distributions of mean age derived from CO_2 and SF_6, J. Geophys. Res., 107 (D12), 4136, doi:10.1029/2001JD000584, 2002.

Engel, A., and Rigby, M. (Lead Authors), Burkholder, J. B., Fernandez, R. P., Froidevaux, L., Hall, B. D., Hossaini, R., Saito, T., Vollmer, M. K., and Yao, B.: Update on Ozone-Depleting Substances (ODSs) and other gases of interest to the Montreal Protocol, Chapter 1 in Scientific Assessment of Ozone Depletion: 2018, Global Ozone Research and Monitoring Project–Report No. 58, World Meteorological Organization, Geneva, Switzerland, 2019.

Eyring, V., Lamarque, J.-F., Hess, P., Arfeuille, F., Bowman, K., Chipperfield, M. P., Duncan, B., Fiore, A., Gettelman, A., Giorgetta, M. A., Granier, C., Hegglin, M., Kinnison, D., Kunze, M., Langematz, U., Luo, B., Martin, R., Matthes, K., Newman, P. A., Peter, T., Robock, A., Ryerson, T., Saiz-Lopez, A., Salawitch, R., Schultz, M., Shepherd, T. G., Shindell, D., Stähelin, J., Tegtmeier, S., Thomason, L., Tilmes, S., Vernier, J.-P., Waugh, D. W., and Young, P. J.: Overview of IGAC/SPARC Chemistry-Climate Model Initiative (CCMI) Community simulations in support of upcoming ozone and climate assessments, SPARC Newsletter, 40, 48–66, 2013.

Haigh, J. D., and Pyle, J. A.: Ozone perturbation experiments in a two-dimensional circulation model, Quart. J. R. Met. Soc., 108, 551-574, 1982.

Hoffmann, L., Hoppe, C. M., Müller, R., Dutton, G. S., Gille, J. C., Griessbach, S., Jones, A. Meyer, C. I., Spang, R., Volk, C. M., and Walker, K. A.: Stratospheric lifetime ratio of CFC-11 and CFC-12 from satellite and model climatologies, Atmos. Chem. Phys., 14, 12479–12497, doi:10.5194/acp-14-12479-2014, 2014.

Hossani, R., Chipperfield, M P., Montzka, S. A., Leeson, A. A., Dhomse, S. S., and Pyle, J. A.: The increasing threat to stratospheric ozone from dichloromethane, Nature Communications, 8:15962, 1–9, doi:10.1038/ncomms15962, 2017.

Jöckel, P., Tost, H., Pozzer, A., Brühl, C., Buchholz, J., Ganzeveld, L., Hoor, P., Kerkweg, A., Lawrence, M. G., Sander, R., Steil, B., Stiller, G., Tanarhte, M., Taraborrelli, D., van Aardenne, J., and Lelieveld, J.: The atmospheric chemistry general circulation model ECHAM5/MESSy1: consistent simulation of ozone from the surface to the mesosphere, Atmos. Chem. Phys., 6, 5067–5104, doi: 10.5194/acp-6-5067-2006, http://www.atmos-chem-phys.net/6/5067/2006/, 2006.

Jöckel, P., Tost, H., Pozzer, A., Kunze, M., Kirner, O., Brenninkmeijer, C. A. M., Brinkop, S., Cai, D. S., Dyroff, C., Eckstein, J., Frank, F., Garny, H., Gottschaldt, K.-D., Graf, P., Grewe, V., Kerkweg, A., Kern, B., Matthes, S., Mertens, M., Meul, S., Neumaier, M., Nützel, M., Oberländer-Hayn, S., Ruhnke, R., Runde, T., Sander, R., Scharffe, D., and Zahn, A.: Earth System Chemistry integrated Modelling (ESCiMo) with the Modular Earth Submodel System (MESSy) version 2.51, Geosci. Model Dev., 9, 1153–1200, https://doi.org/10.5194/gmd-9-1153-2016, http://www.geosci-model-dev.net/9/1153/2016/gmd-9-1153-2016.html, 2016.

Jones, C. D., Hughes, J. K., Bellouin, N., Hardiman, S. C., Jones, G. S., Knight, J., Liddicoat, S., O'Connor, F. M., Andres, R. J., Bell, C., Boo, K.-O., Bozzo, A., Butchart, N., Cadule, P., Corbin, K. D., Doutriaux-Boucher, M., Friedlingstein, P., Gornall, J., Gray, L., Halloran, P. R., Hurtt, G., Ingram, W., Lamarque, J.-F., Law, R. M., Meinshausen, M., Osprey, S., Palin, E., Parsons Chini, L., Raddatz, T., Sanderson, M. G., Sellar, A. A., Schurer, A., Valdes, P., Wood, N., Woodward, S., Yoshioka, M., and Zerroukat, M.: The HadGEM2-ES implementation of CMIP5 centennial simulations, Geosci. Model Dev., 4, 543–570, doi:10.5194/gmd-4-543-2011, 2011.

Kerkweg, A., Sander, R., Tost, H., and Jöckel, P.: Technical note: Implementation of prescribed (OFFLEM), calculated (ONLEM), and pseudo-emissions (TNUDGE) of chemical species in the Modular Earth Submodel System (MESSy), Atmos. Chem. Phys., 6, 3603–3609, doi:10.5194/acp-6-3603-2006, 2006.

Langematz, U., and Tully, M. (Lead Authors), Calvo, N., Dameris, M., de Laat, A. T. J., Klekociuk, A., Müller, R., and Young, P.: Polar stratospheric ozone: past, present, and future, Chapter 4 in Scientific Assessment of Ozone Depletion: 2018, Global Ozone Research and Monitoring Project-Report No. 58, World Meteorological Organization, Geneva, Switzerland, 2019.

Laube, J. C., Newland, M. J., Hogan, C., Brenninkmeijer, C. A. M., Fraser, P. J., Martinerie, P., Oram, D. E., Reeves, C. E., Röckmann, T., Schwander, J. Witrante., and Sturges, W. T. : Newly detected ozone-depleting substances in the atmosphere, Nature Geoscience, 7, 266–269, doi:10.1038/NGEO2109, 2014.

Meul, S., Langematz, U., Oberländer, S., Garny, H., and Jöckel, P.: Chemical contribution to future tropical ozone change in the lower stratosphere, Atmos. Chem. Phys. 14, 2959–2971, doi:10.5194/acp-14-2959-2014, 2014.

Montzka, S. A., Dutton, R., Yu, P., Ray, E., Portmann, R. W., Daniel, J. S., Kuijpers, L., Hall, B. D., Mondeel, D., Siso, C., Nance, D. J., Rigby, M., Manning, A. J., Hu, L., Moore, F., Miller, B. R., Elkins, J. W.: A persistent and unexpected increase in global emissions of ozone-depleting CFC-11, Nature, 557, 413–417, https://doi.org/10.1038/s41586-018-0106-2, 2018.

Rigby, M., Prinn, R. G., O'Doherty, S., Montzka, S. A., McCulloch, A., Harth, C. M., Muhle, J., Salameh, P. K., Weiss, R. F., Young, D., Simmonds, P. G., Hall, B. D., Dutton, G. S., Nance, D., Mondeel, D. J., Elkins, J. W., Krummel, P. B., Steele, L. P. , and Fraser, P. J.: Re-evaluation of the lifetimes of the major CFCs and CH_3CCl_3 using atmospheric trends, Atmos. Chem. Phys., 13, 2691–2702, doi:10.5194/acp-13-2691-2013 , 2013.

van Vuuren, D. P., Edmonds, J., Kainuma, M., Riahi, K., Thomson, A., Hibbard, K., Hurtt, G. C., Kram, T., Krey, V., Lamarque, J.-F., Masui, T., Meinshausen, M., Nakicenovic, N., Smith, S. J., Rose, S. K.: The representative concentration pathways: an overview, Climatic Change, 109, 5–31, doi:10.1007/s10584-011-0148-z, 2011.

WMO (World Meteorological Organization), Scientific Assessment of Ozone Depletion: 2010, Global Ozone Research and Monitoring, Project-Report No. 52, 516 pp., Geneva, Switzerland, 2011.

WMO (World Meteorological Organization), Scientific Assessment of Ozone Depletion: 2018, Global Ozone Research and Monitoring, Project-Report No. 58, 588 pp., Geneva, Switzerland, 2019.

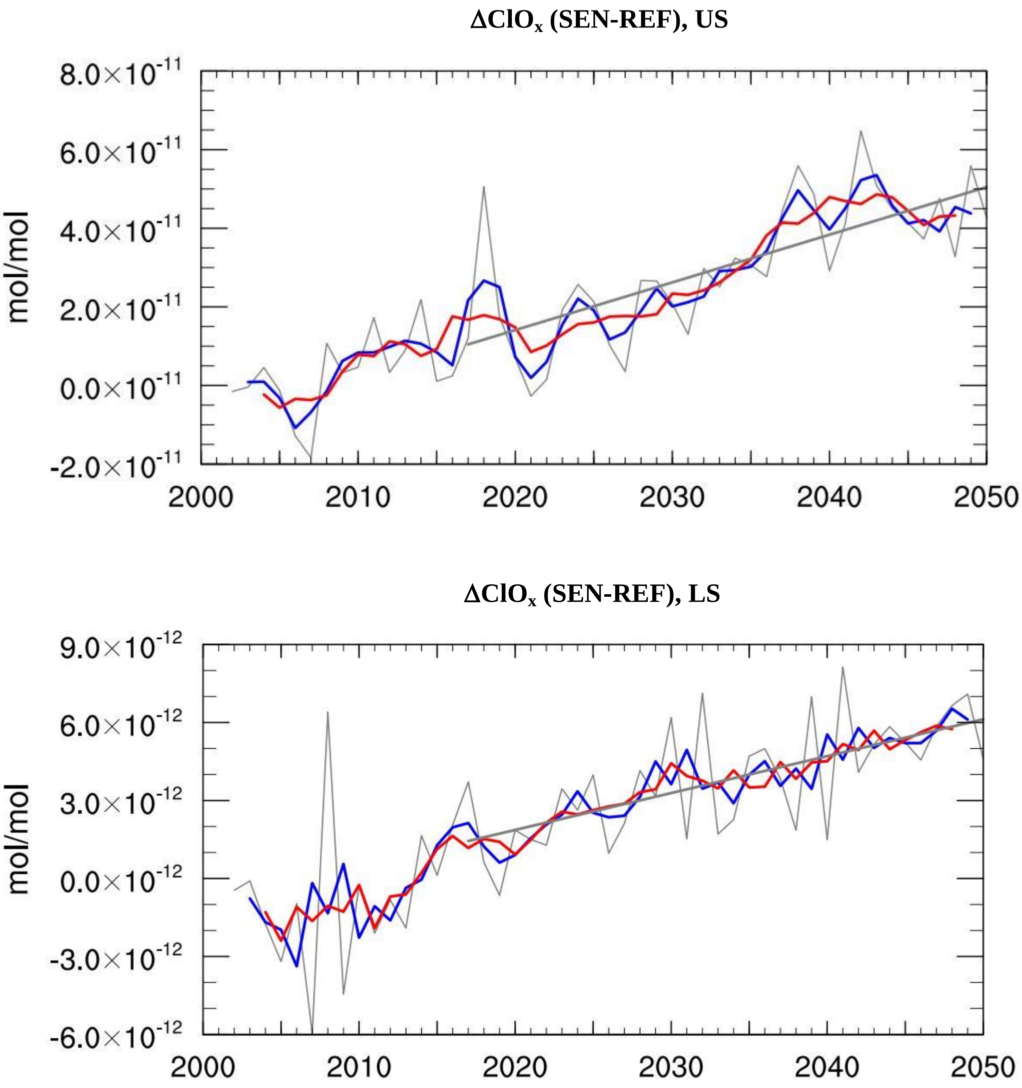

ΔClO$_x$ (SEN-REF), US

ΔClO$_x$ (SEN-REF), LS

Figure 1: Temporal evolution of the annual global mean ClO$_x$ mixing ratio differences (in mol/mol) at around 50 hPa (LS, bottom) and 2 hPa (US, top) between the SEN-C2-fCFC11 and the REF-C2 simulations (i.e. SEN minus REF). The anomalies (here thin grey curves) have been smoothed with a 1-2-1 filter. Red and blue lines show the 3 and 5 year running means, respectively. The dark grey line shows the linear regression estimate between 2017 and 2050.

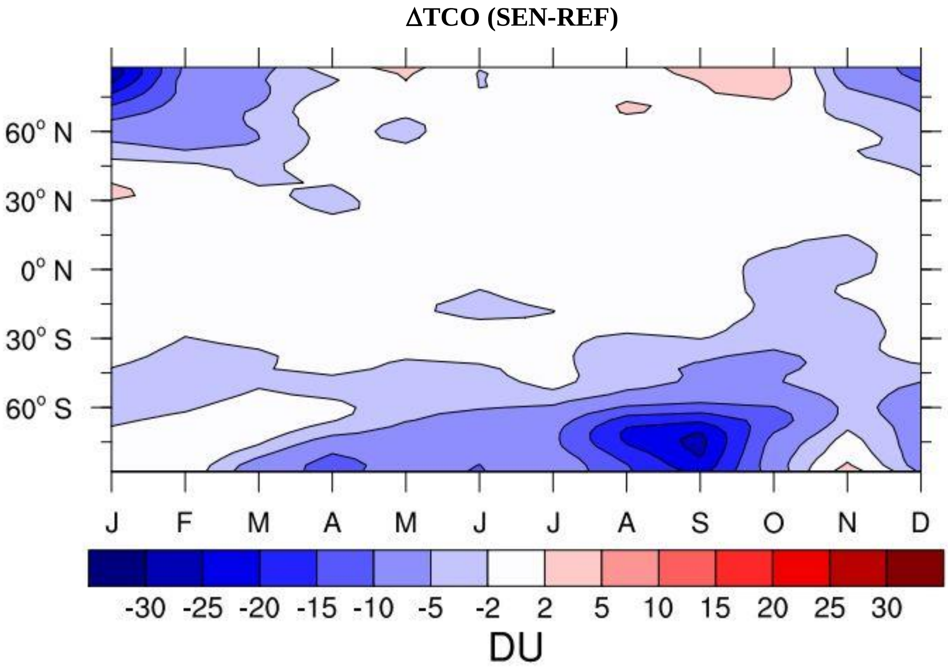

Figure 2: Mean annual cycle of total column ozone (TCO) differences (in Dobson Units, DU) between SEN-C2-fCFC11 and REF-C2 for the 2040s (i.e. SEN minus REF). 5

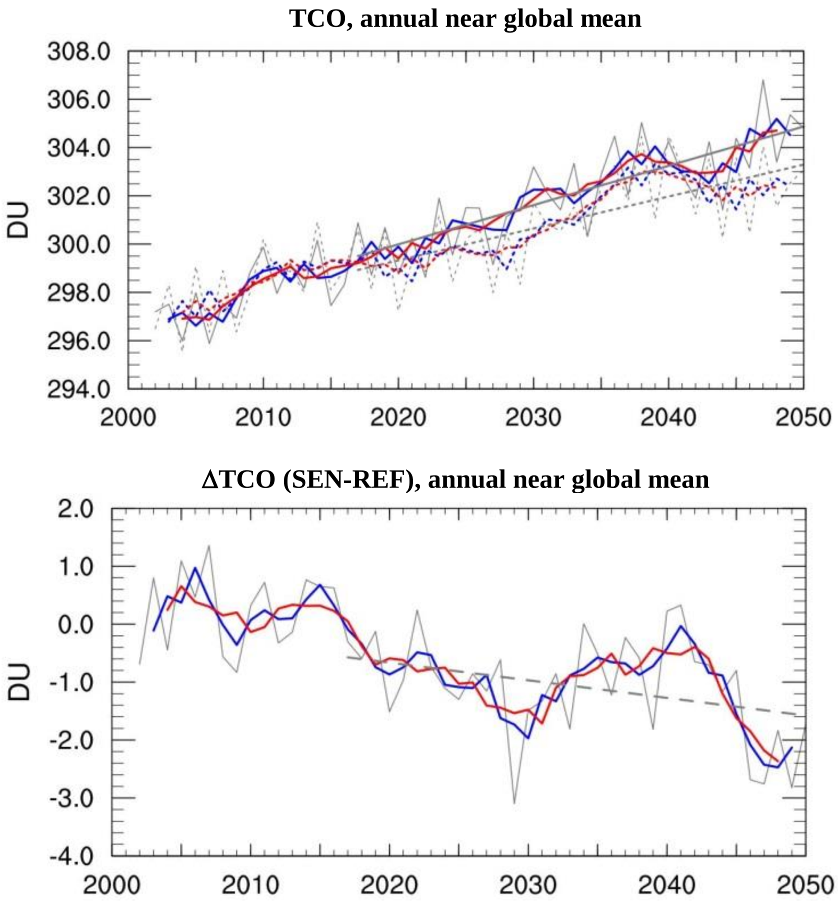

Figure 3: Top: Temporal evolution of total column ozone (TCO; in DU) for the annual near global mean (60° S – 60° N) in REF-C2 (solid grey curve) and in SEN-C2-fCFC11 (dotted grey curves). Bottom: TCO differences (in DU) between SEN-C2-fCFC11 and REF-C2 (i.e. SEN minus REF). Red and blue curves show the 3 and 5 year running means, respectively. The corresponding grey lines (top and bottom) show the respective linear regression estimates between 2017 and 2050.

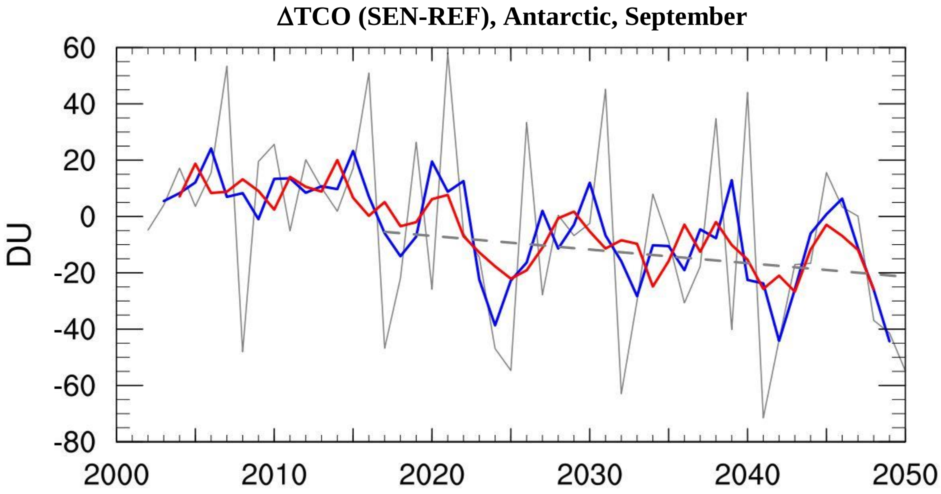

Figure 4: Temporal evolution of TCO differences (in DU) between SEN-C2-fCFC11 and REF-C2 (i.e. SEN minus REF) for the Antarctic region (70° S – 90° S) in September. Red and blue curves show the 3 and 5 year running means, respectively. The corresponding grey dotted line shows the linear regression estimate between 2017 and 2050.

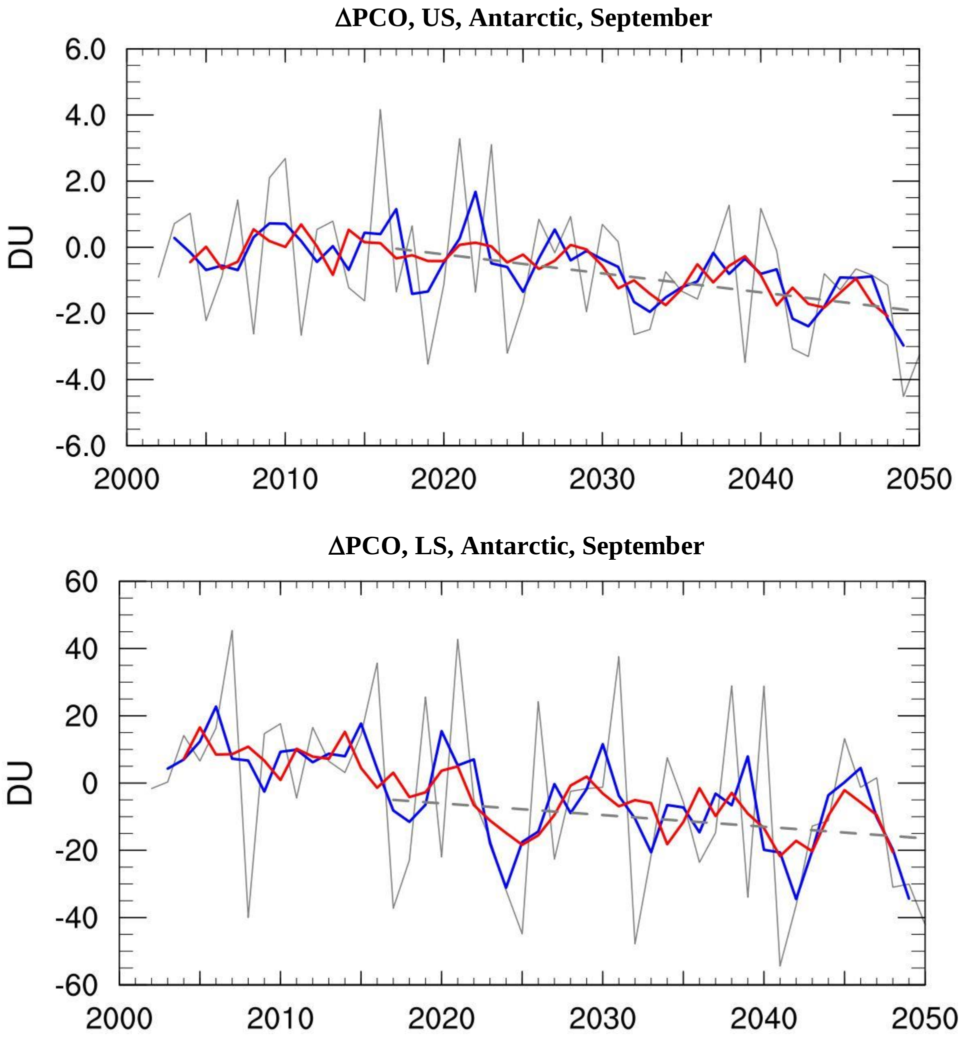

Figure 5: Temporal evolution of Partial Column Ozone (PCO) differences (in DU) between SEN-C2-fCFC11 and REF-C2 (i.e. SEN minus REF) for the Antarctic region (70° S – 90° S) in September. Top: PCO are shown for the US (above 30 km); bottom: PCO are shown for the LS (below 30 km). Red and blue curves show the 3 and 5 year running means, respectively. The corresponding grey dotted line shows the linear regression estimate between 2017 and 2050.

Ozone production rate

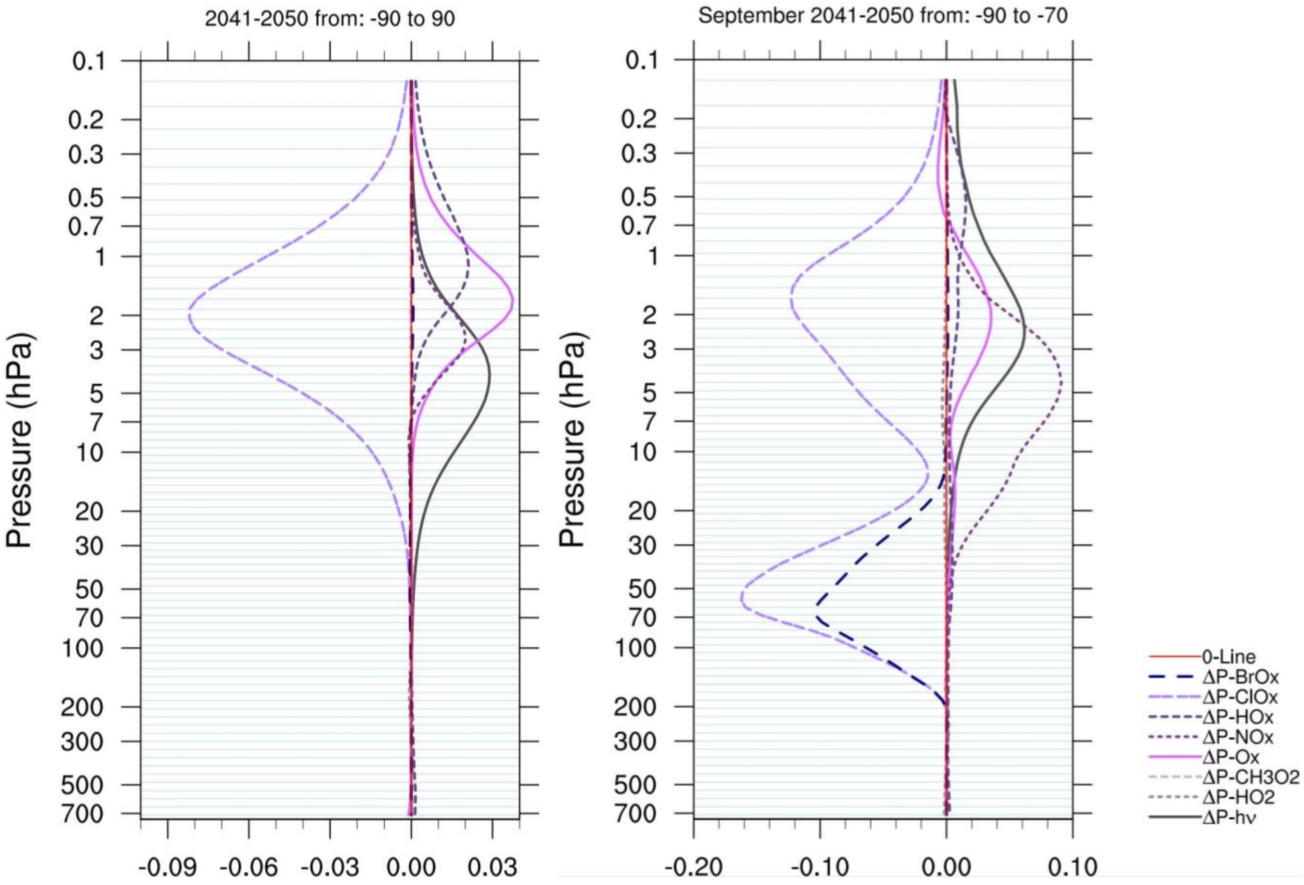

Figure 6: The relative change of ozone production rates (in %), which are normalized to the total column production (through photolysis hυ, HO_2 and CH_3O_2) in the REF-C2 simulation. For the individual ozone destruction cycles and molecules mean difference values are shown, which have been derived from the REF-C2 and the SEN-C2-fCFC11 (i.e. SEN minus REF) simulation for the 2040s (from 2041 to 2050). Left: for the mean annual global mean profiles; right: for the South polar region (70° S – 90° S) in September. Negative values are indicating an intensified ozone loss or a decreased ozone production in the SEN-C2-fCFC11 simulation, whereas higher values indicate more ozone production or less loss through a specific process. Thin horizontal lines indicate the nearest pressure levels to the model grid-boxes.